VOLUME 123, NUMBER 18
MAY 9, 2001

JOURNAL OF THE AMERICAN CHEMICAL SOCIETY

Long-Range Cooperativity in Molecular Recognition of RNA by Oligodeoxynucleotides with Multiple C5-(1-Propynyl) Pyrimidines

Thomas W. Barnes III and Douglas H. Turner*

Contribution from the Department of Chemistry, University of Rochester, Rochester, New York 14627-0216
Received August 29, 2000

Abstract: A heptamer composed of C5-(1-propynyl) pyrimidines (Y^p's) is a potent and specific antisense agent against the mRNA of SV40 large T antigen (Wagner, R. W.; Matteucci, M. D.; Grant, D.; Huang, T.; Froehler, B. C. *Nat. Biotechnol.* **1996**, *14*, 840−844). To characterize the role of the propynyl groups in molecular recognition, thermodynamic increments associated with substitutions in DNA:RNA duplexes, such as 5′-dCCUCCUU-3′:3′-rGAGGAGGAAAU-5′, have been measured by UV melting experiments. For nucleotides tested, an unpaired dangling end stabilizes unmodified and propynylated duplexes similarly, except that addition of a 5′ unpaired rA is 1.4 kcal/mol more stabilizing on the propynylated, PODN:RNA, duplex than on the DNA:RNA duplex. Free energy increments for addition of single propynyl groups range from 0 to −4.0 kcal/mol, depending on the final number and locations of substitutions. A preliminary model for predicting the stabilities of Y^p-containing hybrid duplexes is presented. Eliminating one amino group, and therefore a hydrogen bond, by substituting inosine (I) for guanosine (G), to give 5′-d$C^pC^pU^pC^pC^pU^pU^p$-3′:3′-rGA**GIAGGAA**AU-5′, destabilizes the duplex by 3.9 kcal/mol, compared to 1.7 kcal/mol for the same change within the unpropynylated duplex. This 2.2 kcal/mol difference is eliminated by removing a single propynyl group three base pairs away. CD spectra suggest that single propynyl deletions within the PODN:RNA duplex have position-dependent effects on helix geometry. The results suggest long-range cooperativity between propynyl groups and provide insights for rationally programming oligonucleotides with enhanced binding and specificity. This can be exploited in developing technologies that are dependent upon nucleic acid-based molecular recognition.

Introduction

RNA is a dynamic component of many cellular processes. Consequently, RNA is becoming a target for therapeutics[3] and detection by microarray[4] and molecular beacon[5] technologies. One powerful approach to targeting RNA involves the use of antisense oligonucleotides.[6] In principle, Watson−Crick base-pairing interactions can specifically drive molecular recognition of sense RNA targets by antisense oligonucleotides. Rational design of such therapeutics and probes, however, can be improved by the discovery of new rules for molecular recognition of RNA by antisense compounds. Enhanced understanding

* To whom correspondence should be addressed. E-mail: turner@chem.rochester.edu.

(1) Abbreviations: C^p, C5-(1-propynyl) deoxyribocytidine; C_T, total strand concentration; EDTA, ethylenediaminetetraacetic acid; eu, entropy units (i.e., cal K^{-1} mol^{-1}); I, inosine; IC_{50}, antisense oligomer concentration at which 50% of target's expression is inhibited after microinjection; m-DNA, a DNA containing multiple propynyl substitutions but not fully propynylated; NAED, normalized absolute ellipticity difference; PODN, C5-(1-propynyl) oligodeoxynucleotide; RP-HPLC, reverse-phase high-pressure liquid chromatography; s-DNA, a DNA containing a single propynyl substitution; s-PODN, a PODN containing a single propynyl deletion; TBE, 100 mM Tris, 90 mM boric acid, and 1 mM ethylenediaminetetraacetic acid; T_m, melting temperature in degrees Celsius; T_M, melting temperature in kelvin; U^p, C5-(1-propynyl) deoxyribouridine; Y^p, C5-(1-propynyl)-substituted deoxyribopyrimidine.

(2) Wagner, R. W.; Matteucci, M. D.; Grant, D.; Huang, T.; Froehler, B. C. *Nat. Biotechnol.* **1996**, *14*, 840−844.
(3) Pearson, N. D.; Prescott, N. D. *Chem., Biol.* **1997**, *4*, 409−414.
(4) Schena, M.; Shalon, D.; Davis, R. W.; Brown, P. O. *Science* **1995**, *270*, 467−470.
(5) Leone, G.; van Schijndel, H.; van Gemen, B.; Kramer, F. R.; Schoen, C. D. *Nucleic Acids Res.* **1998**, *26*, 2150−2155.
(6) Zamecnik, P. C.; Stephenson, M. L. *Proc. Natl. Acad. Sci. U.S.A.* **1978**, *75*, 280−284.

10.1021/ja003208t CCC: $20.00
Published on Web 04/11/2001

of nucleic acid interactions can also facilitate design of self-assembling nanostructures based on nucleic acid folding.[7−9]

Studies of the thermodynamic stabilities of nucleic acid duplexes have shown that hydrogen-bonding within Watson−Crick base pairs, and heterocyclic stacking between them, stabilize nucleic acid hybridization.[10,11] The magnitudes of these forces vary due to interactions between "nearest neighbors".[12−14] Extensive studies have elucidated nearest-neighbor parameters of Watson−Crick RNA duplexes,[13] DNA duplexes,[14,15] and DNA:RNA hybrid duplexes.[16,17] On the basis of these and other results, models have been constructed to predict the folding of a given sequence[18] and the optimal unmodified DNA or RNA antisense agents to target a given RNA strand.[19,20]

Advances in synthetic nucleic acid chemistry have provided powerful tools to modify the backbone and heterocyclic bases of nucleic acids, including antisense oligonucleotides.[21] One promising modification that increases antisense target affinity is the substitution of a 1-propynyl functionality at the C5 position of cytosine and uridine, as shown in Figure 1A.[22−24] For example, C5-(1-propynyl) substitutions on pyrimidines can increase the melting temperature, T_m, of a DNA:RNA hybrid by 0.9−2.6 °C per modification.[24,25] C5-(1-propynyl)-substituted pyrimidines (Y^p's) are compatible with modifications along the phosphodiester backbone that increase chemical stability, cellular penetration, and therapeutic potency.[26] Moreover, retaining a deoxyribose sugar allows propynyl-containing oligodeoxynucleotides (PODNs) to induce RNase H hydrolysis of RNA targets,[27] a potent knockout mechanism.[28,29]

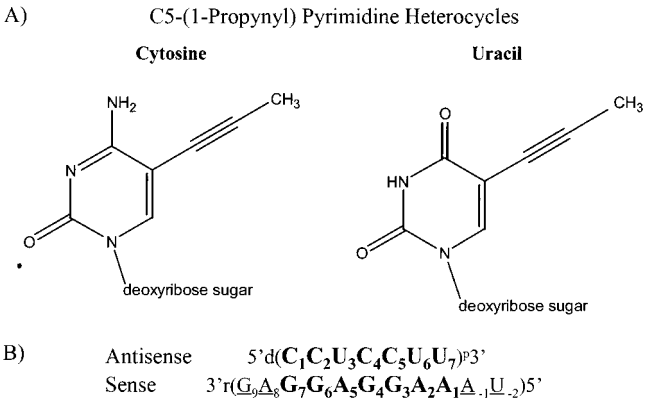

Figure 1. (A) Chemical structures of C5-(1-propynyl)cytosine and C5-(1-propynyl)uracil. (B) Base pairing in the C5-(1-propynyl)oligodeoxyribonucleotide antisense:SV40 TAg mRNA sense complex (GenBank accession no. V01380). This sequence places the sense RNA target (bold) within its natural 5′ and 3′ flanking regions (underlined) of the SV40 TAg mRNA.[2]

The utilization of PODNs as antisense agents in cell cultures has been well documented.[26,27,30] Surprisingly, an antisense PODN heptamer with six phosphorothioate backbone modifications eliminates its SV40 TAg mRNA target with great potency (IC_{50}= 300 nM) and unexpected specificity.[2] The heptamer and its RNA target are shown in Figure 1B. The known properties of PODNs suggest that they may also be useful for designing self-assembling nanostructures.[7−9] Thus, understanding the principles of molecular recognition by PODNs has many applications.

We present a systematic study of the effects of propynylation on the thermodynamics of hybrid duplex formation by the deoxyribonucleotide heptamer shown in Figure 1B. The results reveal non-nearest-neighbor interactions of propynylated pyrimidines that are critically dependent on the number and position of consecutive Y^p's within a PODN strand. A preliminary model is proposed to predict the stabilities of Y^p-containing duplexes. Long-range cooperative interactions apparently contribute 2.6 kcal/mol to the stability of the fully propynylated PODN:RNA duplex at 37 °C. Surprisingly, elimination of a single amino group in the target RNA destabilizes the PODN:RNA complex by 3.9 kcal/mol. Circular dichroism spectra suggest that single propynyl deletions within the PODN:RNA duplex affect helix geometry. The physical forces that dictate these observations are pondered, and the impact of these highly cooperative interactions upon the potency and specificity of PODNs in fields utilizing nucleic acid-based molecular recognition is discussed.

Experimental Section

Oligonucleotide Synthesis and Purification. Riboinosine phosphoramidites were purchased from Chem Genes Corp. All other phosphoramidites and supports were purchased from Glen Research. All oligonucleotides were synthesized[31−33] on an Applied Biosystems 392 DNA/RNA synthesizer using the manufacturer's suggested protocols.

Oligoribonucleotides were deblocked in ethanolic ammonia (1:3 v/v) for 17 h at 55 °C.[34] After the support was filtered away, RNA oligomers

(7) Mirkin, C. A.; Letsinger, R. L.; Mucic, R. C.; Storhoff, J. J. *Nature* **1996**, *382*, 607−609.
(8) Alivisatos, A. P.; Johnsson, K. P.; Peng, X.; Wilson, T. E.; Loweth, C. J.; Bruchez, M. P., Jr.; Schultz, P. G. *Nature* **1996**, *382*, 609−611.
(9) Seeman, N. C. *Annu. Rev. Biomol. Struct.* **1998**, *27*, 225−248.
(10) Burkard, M. E.; Turner, D. H.; Tinoco, I., Jr. In *The RNA World*, 2nd ed.; Gesteland, R. F., Cech, T. R., Atkins, J. F., Eds.; Cold Spring Harbor Laboratory Press: Cold Spring Harbor, NY, 1999; pp 233−264.
(11) Turner, D. H. In *Nucleic Acids: Structures, Properties, and Functions*; Bloomfield, V. A., Crothers, D. M., Tinoco, I., Eds.; University Science Books: Sausolito, CA, 2000; pp 259−336.
(12) Borer, P. N.; Dengler, B.; Tinoco, I., Jr.; Uhlenbeck, O. C. *J. Mol. Biol.* **1974**, *241*, 246−262.
(13) Xia T.; SantaLucia J., Jr.; Burkard M. E.; Kierzek R.; Schroeder S. J.; Jiao X.; Cox C.; Turner D. H. *Biochemistry* **1998**, *42*, 14719−14735.
(14) SantaLucia, J., Jr. *Proc. Natl. Acad. Sci. U.S.A.* **1998**, *95*, 1460−1465.
(15) SantaLucia, J., Jr.; Allawi, H. T.; Seneviratne, P. A. *Biochemistry* **1996**, *35*, 3555−3562.
(16) Sugimoto N.; Nakano S.; Katoh M.; Matsumura A.; Nakamuta H.; Ohmichi T.; Yoneyama M.; Sasaki M. *Biochemistry* **1995**, *34*, 11211−11216.
(17) Gray, D. *Biopolymers* **1997**, *42*, 795−810.
(18) Mathews D. H.; Sabina J.; Zuker M.; Turner D. H. *J. Mol. Biol.* **1999**, *288*, 911−940.
(19) Mathews, D. H.; Burkard, M. E.; Freier, S. M.; Wyatt, J. R.; Turner, D. H. *RNA* **1999**, *5*, 1458−1469.
(20) Walton, S. P.; Stephanopoulos, G. N.; Yarmush, M. L.; Roth, C. M. *Biotechnol. Bioeng.* **1999**, *65*, 1−9.
(21) Verma, S.; Eckstein, F. *Annu. Rev. Biochem.* **1998**, *67*, 99−134.
(22) De Clercq, E.; Descamps, J.; Balzarini, J.; Giziewicz, J.; Barr, P. J.; Robins, M. J. *J. Med. Chem.* **1983**, *26*, 661−666.
(23) Hobbs, F. W. *J. Org. Chem.* **1989**, *54*, 3420−3422.
(24) Froehler, B. C.; Wadwani, S.; Terhorst, T. J.; Gerrard, S. R. *Tetrahedron Lett.* **1992**, *33*, 5307−5310.
(25) Freier, S. M.; Altmann, K. H. *Nucleic Acids Res.* **1997**, *25*, 4429−4443.
(26) Wagner, R. W.; Matteucci, M. D.; Lewis, J. G.; Gutierrez, A. J.; Moulds, C.; Froehler, B. C. *Science* **1993**, *260*, 1510−1513.
(27) Moulds, C.; Lewis, J. G.; Froehler, B. C.; Grant D.; Huang T.; Milligan, J. F.; Matteucci, M. D.; Wagner, R. W. *Biochemistry* **1995**, *34*, 5044−5053.
(28) Bonham M. A.; Brown S.; Boyd A. L.; Brown P. H.; Bruckenstein D. A.; Hanvey J. C.; Thomson S. A.; Pipe A.; Hassman F.; Bisi J. E.; et al. *Nucleic Acids Res.* **1995**, *23*, 1197−1203.
(29) Gee, J. E.; Robbins, I.; van der Laan, A. C.; van Boom, J. H.; Colombier, C.; Leng, M.; Raible, A. M.; Nelson, J. S.; Lebleu, B. *Antisense Nucleic Acid Drug Dev.* **1998**, *8*, 103−111.
(30) Flanagan, W. M.; Kothavale, A.; Wagner, R. W. *Nucleic Acids Res.* **1996**, *24*, 2936−2941.
(31) Matteucci, M. D.; Caruthers, M. H. *Biotechnology* **1981**, *24*, 92−98.
(32) Usman, N.; Ogilvie, K. K.; Jiang, M.-V.; Cedergren, R. *J. Am. Chem. Soc.* **1987**, *109*, 7845−7854.
(33) Wincott, F.; DiRenzo, A.; Shaffer, C.; Grimm, S.; Tracz, D.; Workman, C.; Sweedler, D.; Gonzalez, C.; Scaringe, S.; Usman, N. *Nucleic Acids Res.* **1995**, *23*, 2677−2684.
(34) Stawinski, J.; Strömberg, R.; Thelin, M.; Westman, E. *Nucleosides Nucleotides* **1988**, *7*, 779−782.

were incubated in 1 M triethylammonium hydrogen fluoride (50 equiv) at 55 °C for 50 h. Solutions of crude products were evaporated, dissolved in water, and extracted against diethyl ether. After removal of residual ether by evaporation, 5 mM aqueous ammonium acetate (pH = 7.0) was added, and the oligomers were desalted on a reverse-phase Sep-Pak C-18 cartridge (Waters Corp.). The oligomers were purified by 20% PAGE. The product was UV-visualized, cut out, and eluted with sterile water containing 0.5 mM Na_2EDTA. After being separated from a majority of the urea with a prepacked PD-10 Sephadex column (Amersham Pharmacia Biotech), the samples were dialyzed in an irradiated cellulose ester (MWCO = 1000) Spectra/Por Dispodialyzer (Spectrum Labs Inc.) against 0.1 mM EDTA (pH = 7.0) and subsequently against sterile water. Samples were then lyophilized.

To test purity, RNA oligomers were 5′-radiolabeled by incubating 2.4 pmol of RNA and 30 pmol of [γ-^{32}P]ATP (New England Nuclear) in 7.5 μL of 50 mM Tris (pH = 7.5), 10 mM $MgCl_2$, 5 mM DTT, 0.1 mM spermidine, and 0.1 mM Na_2EDTA with 7.5 units of T4 polynucleotide kinase (Gibco-BRL) at 37 °C. After 10 min, the reaction was stopped with 7.5 μL of 2X stop buffer (10 M urea, 10 mM EDTA, pH = 7.0) and applied to a 20% polyacrylamide, 8 M urea denaturing gel for electrophoresis with 1X TBE running buffer. Once bromophenol blue dye reached 18 cm, the products were imaged and quantified with a Molecular Dynamics phosphorimager and quantitation software package. Purity was greater than 95%. Product identity was confirmed for all RNA strands by electrospray mass spectroscopy on an Hewlett-Packard G1946 LC/MS instrument.

The 5′-trityl oligodeoxynucleotides and C5-(1-propynyl)-5′-trityl-oligodeoxynucleotides were incubated in concentrated ammonium hydroxide at 55 °C for 2 h. After the support was removed by spin filtration, the crude product was applied to, and eluted from, a Poly Pak II cartridge (Glen Research) using the manufacturer's recommended protocol to purify the desired product from most of the failure sequences. The product was further purified by preparative thin-layer chromatography (TLC) with an *n*-propanol:ammonium hydroxide:water (55:35:10) running buffer. Reverse-phase C-18 Sep-Pak cartridges (Waters Corp.) were used to desalt the products, which were then lyophilized. The purity of all PODNs and DNAs was greater than 95% on the basis of RP-HPLC on a SUPELCOSIL ABZ+ Plus semi-preparative column (Supelco) with a gradient from 0 to 30% acetonitrile (by volume) in 100 mM aqueous triethylamine acetate (pH = 7.0) over 1 h at a flow rate of 1 mL/min. Product identity of the DNA and PODN strands was confirmed by electrospray mass spectroscopy. Likewise, the identities of over half of the sequences within the s-DNA, s-PODN, and m-DNA families were tested and confirmed.

UV Melting. Thermodynamic parameters were measured in 1.0 M NaCl, 0.5 mM Na_2EDTA, 20 mM sodium cacodylate at a pH of 7.0. Single-strand oligoribonucleotide concentrations were calculated from high-temperature absorbances at 280 nm and predicted single-strand extinction coefficients.[35,36] Single-strand DNA concentrations were determined from high-temperature absorbances at 260 nm on the basis of monomer extinction coefficients.[37] Single-strand PODN concentrations were calculated from high-temperature absorbances at 260 nm on the basis of monomer extinction coefficients of 3200 and 5000 M^{-1} cm^{-1} for U^p and C^p, respectively (generously provided by M. D. Matteucci and B. C. Froehler). These were also used in conjunction with DNA monomer extinction coefficients at 260 nm to estimate the concentrations of chimera oligomers containing modified and unmodified pyrimidines.

Appropriate single strands were mixed at 1:1 concentration ratios, denatured for 1 min at 90 °C, and reannealed by slow cooling to 0 °C. UV melting curves were measured at 280 nm with a heating rate of 1 °C/min on a Gilford 250 spectrophotometer. Each melting curve was fit to a non-self-complementary two-state model[38] with the Meltwin software package.[39] The thermodynamic parameters were averaged over all melts of a given duplex and compared to those generated by plotting the reciprocal of the melting temperature, T_M^{-1}, versus $\log(C_T/4)$, where C_T is the total concentration of strands:[12]

$$T_M^{-1} = (2.303R/\Delta H^\circ)\log(C_T/4) + \Delta S^\circ/\Delta H^\circ \quad (1)$$

With only two minor exceptions (5′dC^{p}C^{p}U^{p}C^{p}C^{p}U^{p}U^{p}C^{p}3′:3′rGGAGGAA5′ and 5′dCCUCCUU3′:3′r<u>GA</u>**GIAGGAA**<u>AU</u>5′), the enthalpy changes generated from the two methods of data analysis agree within 15%, consistent with two-state melting.[40] Errors were calculated as in Xia et al.[13] and references therein. When comparing the thermodynamic parameters of two different hybrid systems, the T_M^{-1} versus $\log[C_T/4]$ results were used. The fitting procedure neglects any heat capacity change associated with the reaction, and this introduces additional error in the derived ΔH°.[41] Smaller errors are introduced into ΔG°, however, due to compensating errors in ΔS°.

Multiple Linear Regression and Statistical Analyses. Using Microsoft Excel software, linear regression analysis[42,43] of the measured ΔG°_{37} values was used to determine parameters for models to predict the stabilities of Y^p-containing DNA:RNA duplexes. The sample data set contains only 22 duplexes. Therefore, the Student's *t*-test was used to determine whether each parameter is statistically significant.[44]

Circular Dichroism (CD) Measurements. CD spectra of duplexes were measured on a Jasco J-710 spectropolarimeter in a cell with path length, *L*, of 1 cm. Data were collected at 0.1 nm intervals, at a scan speed of 10 nm/min. Sample temperatures were maintained at 20 °C by a water bath as five scans were collected and averaged. The molar ellipticity, $[\theta]$, was calculated from the observed ellipticity, θ, and duplex concentration, *c*:

$$[\theta] = \theta/cL \quad (2)$$

Results

PODN:RNA vs DNA:RNA Duplex Stability. Thermodynamic parameters were measured for duplex formation between the DNA, d(5′CCUCCUU3′), or its fully propynylated analogue and an RNA 7-mer, r(3′GGAGGAA5′), that can form the same base pairs as the target sequence within the SV40 TAg mRNA (Figure 1B). Figure 2 shows representative melt curves and van't Hoff plots of the DNA:RNA 7-mer and PODN:RNA 7-mer duplexes. Full propynylation has a dramatic effect on duplex stability, ΔG°_{37}(DNA:RNA 7-mer) = −7.6 kcal/mol, whereas ΔG°_{37}(PODN:RNA 7-mer) = −15.3 kcal/mol (Table 1). Thus, full propynylation increases the equilibrium constant for duplex formation by more than 200 000-fold at 37 °C.

The T_M of the PODN:RNA 7-mer duplex at 10^{-4} M strand concentration is 31 K higher than that of the unpropynylated duplex. If there is a heat capacity change associated with duplex formation, then ΔH° and ΔS° will be temperature-dependent:[45]

$$d\Delta H^\circ/dT = \Delta C^\circ_p \quad (3)$$

$$d\Delta S^\circ/d\ln(T) = \Delta C^\circ_p \quad (4)$$

This temperature dependence can skew thermodynamic com-

(35) Borer, P. N. In *Handbook of Biochemistry and Molecular Biology: Nucleic Acids*, 3rd ed.; Fasman, G. D., Ed.; CRC Press: Cleveland, OH, 1975; Vol. I, p 589.
(36) Richards, E. G. In *Handbook of Biochemistry and Molecular Biology: Nucleic Acids*, 3rd ed.; Fasman, G. D., Ed.; CRC Press: Cleveland, OH, 1975; Vol. I, p 597.
(37) Puglisi, J. D.; Tinoco, I., Jr. *Methods Enzymol.* **1989**, *180*, 304−325.
(38) Longfellow, C. E.; Kierzek, R.; Turner, D. H. *Biochemistry* **1990**, *29*, 278−285.
(39) McDowell, J. A.; Turner, D. H. *Biochemistry* **1996**, *35*, 14077−14089.
(40) Freier, S. M.; Kierzek, R.; Jaeger, J. A.; Sugimoto, N.; Caruthers, M. H.; Neilson, T.; Turner, D. H. *Proc. Natl. Acad. Sci. U.S.A.* **1986**, *83*, 9373−9377.
(41) Chaires, J. B. *Biophys. Chem.* **1997**, *64*, 15−23.
(42) Seber, G. A. F. *Linear Regression Analysis*; John Wiley & Sons: New York, 1977.
(43) Neter, J.; Wasserman, W.; Kutner, M. H. *Applied Statistical Models*, 2nd ed.; Richard D. Irwin, Inc.: Homewood, IL, 1985.
(44) Meyer, S. L. *Data Analysis for Scientists and Engineers*; Wiley & Sons: New York, 1975.
(45) Lewis, G. N.; Randall, M. *Thermodynamics*, 2nd ed.; Revised by Pitzer, K. S., Brewer, L.; McGraw-Hill: New York, 1961.

Table 1. Thermodynamic Parameters of DNA:RNA and PODN:RNA Hybrid Duplexes Containing Various 5′ and 3′ Dangling Ends[a]

		$1/T_M$ plots			
	reference symbol	$\Delta G°_{37}$ (kcal/mol)	$\Delta H°$ (kcal/mol)	$\Delta S°$ (kcal/mol)	T_m (°C)[b]
		d(5′CCUCCUU3′)			
r(3′GGAGGAA5′)	7-mer	−7.6 ± 0.1	−53.3 ± 2.0	−147.3 ± 6.4	43.3
r(3′AGGAGGAA5′)	8-mer	−8.9 ± 0.1	−61.2 ± 1.8	−168.6 ± 5.7	49.3
r(3′AGGAGGAAA5′)	9-mer	−9.4 ± 0.2	−62.0 ± 2.4	−169.7 ± 7.1	52.0
		d(5′C^{p}C^{p}U^{p}C^{p}C^{p}U^{p}U^{p}3′)			
r(3′GGAGGAA5′)	7-mer	−15.3 ± 0.4	−80.9 ± 4.0	−211.6 ± 11.3	74.5
r(3′AGGAGGAA5′)	8-mer	−16.2 ± 0.6	−79.0 ± 5.2	−200.4 ± 14.7	80.2
r(3′AGGAGGAAA5′)	9-mer	−18.2 ± 0.3	−89.0 ± 3.1	−228.5 ± 10.8	83.6
		r(3′GGAGGAA5′)			
d(5′CCCUCCUU3′)	DNA-5′C	−8.3 ± 0.1	−56.1 ± 3.0	−154.2 ± 9.6	46.9
d(5′CCUCCUUC3′)	DNA-3′C	−7.8 ± 0.1	−51.4 ± 2.1	−140.7 ± 6.8	44.8
d(5′C^{p}C^{p}C^{p}U^{p}C^{p}C^{p}U^{p}U^{p}U^{p}3′)	PODN-5′C^p	−15.6 ± 0.4	−79.6 ± 3.4	−206.2 ± 9.9	76.9
d(5′C^{p}C^{p}U^{p}C^{p}C^{p}U^{p}U^{p}C^{p}3′)	PODN-3′C^p	(−16.0 ± 0.4)	(−88.0 ± 3.6)	(−232.3 ± 10.5)	74.4

[a] Measured in 1.0 M NaCl, 0.05 mM Na_2EDTA, 20 mM sodium cacodylate, pH 7. Values in parentheses indicate that the $\Delta H°$ values determined from T_M^{-1} vs $\ln(C_T/4)$ plots and from curve fitting differ by more than 15%, thus indicating non-two-state melting. For all sequences, parameters from curve fitting are given in the Supporting Information. Errors are based on the standard deviations of the thermodynamic parameters and were calculated as described in ref 13. Errors from all sources are estimated as ±10%, ±10%, and ±5% for $\Delta H°$, $\Delta S°$, and $\Delta G°_{37}$, respectively. Significant figures are given beyond error estimates to allow accurate calculation of T_M and other parameters. [b] T_M for a total strand concentration of 1×10^{-4} M.

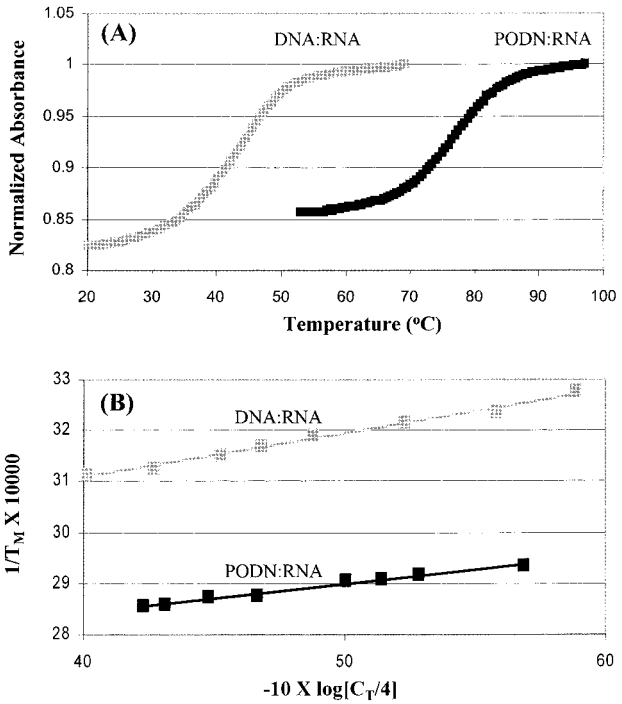

Figure 2. (A) Representative normalized UV melting curves at 280 nm of the DNA:RNA (gray) and PODN:RNA (black) duplexes at about 10 μM strand concentration. (B) Representative plots of the reciprocal of melting temperature versus log concentration for the DNA:RNA (gray) and PODN:RNA (black) hybrid duplexes. The concentration range for the PODN:RNA complex is smaller than that of the DNA:RNA complex because high concentrations of the PODN:RNA hybrid have T_M values that are too high to measure accurately.

parisons of systems with very different T_M values. To take $\Delta C°_p$ into account when comparing the DNA:RNA 7-mer and PODN:RNA 7-mer duplexes at 37 °C, plots of $\Delta H°$ vs T_M and $\Delta S°$ vs $\ln(T_M)$ were generated (Figure 3). The slope of each plot provides the $\Delta C°_p$ of duplex formation. The average $\Delta C°_p$ values of the DNA:RNA 7-mer and PODN:RNA 7-mer duplexes are −0.86 and −0.44 kcal/(mol K), respectively (Table 2). On a per nucleotide basis, these values are similar to those reported for duplex formation by other nucleic acids.[46−49]

The $\Delta C°_p$ values allow extrapolation of the $\Delta H°$ and $\Delta S°$ values to any temperature. The $\Delta H°$ values for the DNA:RNA 7-mer and PODN:RNA 7-mer duplexes at 37 °C are −54.5 and −44.1 kcal/mol, respectively (Table 2). The $\Delta S°$ values for the DNA:RNA 7-mer and PODN:RNA 7-mer duplexes at 37 °C are −151.4 and −90.9 eu, respectively (Table 2). From these results, the $\Delta G°_{37}$ values of the DNA:RNA 7-mer and PODN:RNA 7-mer duplexes are −7.5 and −15.9 kcal/mol, which correspond well with those derived from T_M^{-1} vs $\log[C_T/4]$ plots (Table 1). The consideration of heat capacity affects the difference in $\Delta G°_{37}$ only marginally, even though the differences in $\Delta H°$ and $\Delta S°$ are reduced and change sign (Tables 1 and 2). When the effect of $\Delta C°_p$ is considered, the propynylated duplex has a less favorable enthalpy change and a more favorable entropic penalty for formation than the unpropynylated duplex.

The average T_m values of the DNA:RNA and PODN:RNA melts are 41.0 and 72.8 °C, respectively (Figure 2B). Thus, a much shorter extrapolation to 37 °C is required for the DNA:RNA than the PODN:RNA duplex. This difference could skew the quantitative comparison of $\Delta H°$ and $\Delta S°$ values at 37 °C. To minimize this effect, thermodynamic parameters were also extrapolated to 56.9 °C, half way between the average T_m values of the two data sets (Table 2). At 56.9 °C the enthalpy change for PODN:RNA 7-mer formation is also more unfavorable and the entropy change more favorable relative to DNA:RNA 7-mer formation. This suggests that any errors in the $\Delta H°$ and $\Delta S°$ values, resulting from large extrapolations, do not affect qualitative comparisons at 37 °C.

Effects of 5′ and 3′ Terminal Unpaired Adenosines in the RNA Strand on Hybrid Duplex Stability. To provide an empirical measure of stacking interactions possible for rA's in a duplex containing an all-purine RNA strand and an all-pyrimidine DNA strand, duplex stabilities were measured for d(5′CCUCCUU3′):r(3′AGGAGGAA5′), d(5′CCUCCUU3′):r(3′AGGAGGAAA5′), and their fully propynylated analogues. The underlined rA's are unpaired. The results in Table 1 allow

(46) Petersheim, M.; Turner, D. H. *Biochemistry* **1983**, *22*, 256−263.
(47) Freier, S. M.; Alkema, D.; Sinclair, A.; Neilson, T.; Turner, D. H. *Biochemistry* **1985**, *24*, 4533−4539.
(48) Chalikian, T. V.; Volker, J.; Plum, G. E.; Breslauer, K. J. *Proc. Natl. Acad. Sci. U.S.A.* **1999**, *96*, 7853−7858.
(49) Holbrook, J. A.; Capp, M. W.; Saecker, R. M.; Record, M. T., Jr. *Biochemistry* **1999**, *38*, 8408−8422.

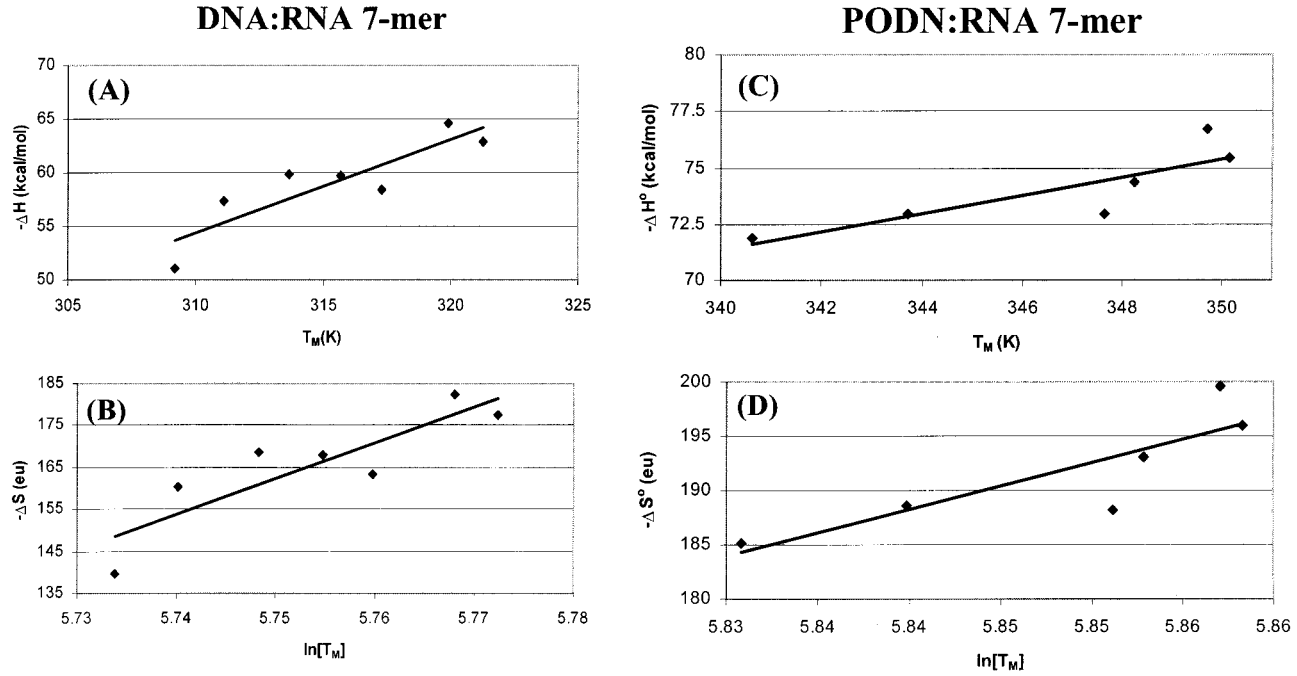

Figure 3. Plots of $\Delta H°$ vs T_M and $\Delta S°$ vs $\ln(T_M)$ for the 5′-dCCUCCUU-3′:3′-rGGAGGAA-5′ and 5′-dC^{p}C^{p}U^{p}C^{p}C^{p}U^{p}U^p-3′:3′-rGGAGGAA-5′ duplexes. The R^2 values of these plots are (A) 0.72, (B) 0.73, (C) 0.77, and (D) 0.76.

Table 2. $\Delta C°_p$, $\Delta H°$, $\Delta S°$, and $\Delta G°_{37}$ Comparison[a]: DNA:RNA[b] vs PODN:RNA[b]

	$\Delta C°_p$ (kcal mol^{-1} K^{-1})	$\Delta H°$ (kcal/mol)	$\Delta S°$ (eu)	$\Delta G°$ (kcal/mol)
DNA:RNA	-0.86^c $(0.85)^d \pm 0.21$	-54.5^e $(71.7)^h$	-151.4^e $(204.2)^h$	-7.54^g $(4.3)^j$
PODN:RNA	$-0.41^c$$(0.48)^d \pm 0.14$	-44.1^f $(52.2)^i$	-90.9^f $(120.3)^i$	-15.9^g $(12.5)^j$

[a] From data in Figure 3. [b] RNA is 3′-rGGAGGAA-5′. [c] Slope of linear fits of $-\Delta H°$ vs T_M. [d] Slope of linear fits of $-\Delta S°$ vs $\ln[T_M]$. [e] From interpolation at 37 °C of linear fits in Figures 3A,B. [f] From extrapolation to 37 °C of linear fits in Figures 3C,D. [g] Calculated at 37 °C from $\Delta H°$ and $\Delta S°$. [h] From extrapolation to 56.9 °C of linear fits in Figures 3A,B. [i] From extrapolation to 56.9 °C of linear fits in Figures 3C,D. [j] Calculated from $\Delta H°$ and $\Delta S°$ at 56.9 °C.

Table 3. Free Energies at 37 °C of 5′- and 3′-Terminal Unpaired Nucleotides[a]

5′ stack	$\Delta G°_{37}$ (kcal/mol)	3′ stack	$\Delta G°_{37}$ (kcal/mol)
5′dAA/dU	-0.5^b	dC/dGA3′	-0.4^b
5′rAA/rU	-0.3^c	rC/rGA3′	-1.1^c
5′rAA/dU	−0.5	dC/rGA3′	−1.3
5′rAA/dU^p	−1.9	dC^p/dGA3′	−0.9
5′dCC/dG	-0.5^b	dA/dTC3′	-0.2^b
5′rCC/rG	-0.3^c	rA/rUC3′	-0.1^c
5′dCC/rG	−0.7	rA/dUC3′	−0.2
5′dC^{p}C^p/rG	−0.3	rA/dUC^{p}3′	−0.7

[a] Underlined nucleotides are unpaired dangling ends. [b] From ref 65. [c] From refs 11, 46, and 64.

calculation of free energy increments for the unpaired nucleotides:

$$\Delta\Delta G°_{37}(3'\text{A}) = \Delta G°_{37}(\text{DNA:RNA 8-mer}) - \Delta G°_{37}(\text{DNA:RNA 7-mer}) \quad (5)$$

$$\Delta\Delta G°_{37}(5'\text{A}) = \Delta G°_{37}(\text{DNA:RNA 9-mer}) - \Delta G°_{37}(\text{DNA:RNA 8-mer}) \quad (6)$$

These increments are listed in Table 3. At 37 °C, a 5′ dangling rA on a DNA:RNA helix stabilizes the duplex by 0.5 kcal/mol, and a 3′ dangling rA stabilizes it by 1.3 kcal/mol. On a fully propynylated PODN:RNA duplex, however, they stabilize by 1.9 and 0.9 kcal/mol, respectively. Therefore, a 3′ unpaired rA is more stabilizing than a 5′ unpaired rA in the unmodified duplex, while the reverse is true in the propynylated duplex.

Effects of 5′ and 3′ Terminal Unpaired Cytosines in the DNA or PODN Strand on Hybrid Duplex Stability. To provide an empirical measure of stacking interactions possible for dC's in a duplex containing an all-purine RNA strand and an all-pyrimidine DNA strand, duplex stabilities were measured for d(5′CCCUCCUU3′):r(3′GGAGGAA5′), d(5′CCUCCUUC3′):r(3′GGAGGAA5′) and their fully propynylated analogues (Table 1). The underlined dC's are unpaired. Table 3 lists the free energy increments calculated by analogy to eq 5. An unmodified deoxycytidine stacking on the 5′ or 3′ end of the unmodified DNA:RNA helix stabilizes duplex formation by 0.7 and 0.2 kcal/mol, respectively, while a dC^p stacking on the 5′ or 3′ end of the fully modified PODN:RNA helix stabilizes duplex formation by 0.3 and 0.7 kcal/mol, respectively. Thus, effects of propynylation on stacking of dC are relatively small, and the dangling end providing more stabilization appears to switch from 5′ to 3′.

Effects of Adding More Unpaired Dangling Nucleotides to the 5′ and 3′ ends of the RNA Strand in the Hybrid Duplex. The RNA 11-mer, r(3′GA**GGAGGAA**AU5′), was selected as the RNA strand for additional experiments because it places the target sequence within its naturally occurring flanking nucleotides of the SV40 TAg mRNA (Figure 1) and because it has been used as the mimic in previous studies.[50] Addition of the 5′-terminal U and the 3′-terminal G unpaired nucleotides to the duplex has little effect on stability. The $\Delta G°_{37}$(PODN:RNA 9-mer) and $\Delta G°_{37}$(PODN:RNA 11-mer) values are −18.2 and −18.4 kcal/mol, respectively, and $\Delta G°_{37}$(DNA:RNA 9-mer) and $\Delta G°_{37}$(DNA:RNA 11-mer) are −9.4 and −9.6

(50) Flanagan, W. M.; Wagner, R. W.; Grant, D.; Lin, K. Y.; Matteucci, M. D. *Nat. Biotechnol.* **1999**, *17*, 48−52.

Table 4. Thermodynamic Parameters of the DNA, s-DNAs, PODN, and s-PODNs Bound to 3′-rGAGGAGGAAAU-5′ [a,b]

		$1/T_M$ plots			
	reference symbol	$\Delta G°_{37}$ (kcal/mol)	$\Delta H°$ (kcal/mol)	$\Delta S°$ (eu)	T_m (°C)
d(5′CCUCCUU3′)	DNA	−9.6 ± 0.1	−62.8 ± 1.7	−171.4 ± 4.9	53.0
d(5′**C**^{p}CUCCUU3′)	s-DNA1	−9.6 ± 0.1	−65.6 ± 2.7	−180.7 ± 8.4	52.2
d(5′C**C**^{p}UCCUU3′)	s-DNA2	−10.0 ± 0.1	−61.0 ± 2.0	−164.4 ± 6.0	55.7
d(5′CC**U**^{p}CCUU3′)	s-DNA3	−10.1 ± 0.1	−64.0 ± 1.5	−173.7 ± 4.7	55.2
d(5′CCU**C**^{p}CUU3′)	s-DNA4	−10.6 ± 0.2	−68.2 ± 3.7	−185.7 ± 11.4	56.7
d(5′CCUC**C**^{p}UU3′)	s-DNA5	−10.2 ± 0.1	−61.6 ± 2.3	−165.7 ± 7.1	56.6
d(5′CCUCC**U**^{p}U3′)	s-DNA6	−9.8 ± 0.1	−61.2 ± 1.8	−165.7 ± 5.5	54.6
d(5′CCUCCU**U**^{p}3′)	s-DNA7	−9.6 ± 0.1	−62.0 ± 2.0	−169.6 ± 6.2	52.0
d(5′CUCCUU3′)	DNA 6-mer	−6.7 ± 0.1	−52.8 ± 1.9	−148.5 ± 6.3	38.1
d(5′C^{p}U^{p}C^{p}C^{p}U^{p}U^{p}3′)	PODN 6-mer	−13.8 ± 0.3	−75.8 ± 2.8	−199.9 ± 8.1	70.1
d(5′C^{p}C^{p}U^{p}C^{p}C^{p}U^{p}U^{p}3′)	PODN	−18.4 ± 0.6	−89.3 ± 5.4	−228.7 ± 15.5	84.3
d(5′**C**C^{p}U^{p}C^{p}C^{p}U^{p}U^{p}3′)	s-PODN1	−15.2 ± 0.3	−71.1 ± 2.9	−180.2 ± 8.4	79.9
d(5′C^p**C**U^{p}C^{p}C^{p}U^{p}U^{p}3′)	s-PODN2	−14.8 ± 0.2	−70.8 ± 2.0	−180.6 ± 4.9	78.2
d(5′C^{p}C^p**U**C^{p}C^{p}U^{p}U^{p}3′)	s-PODN3	−14.4 ± 0.2	−67.4 ± 3.9	−171.0 ± 11.0	77.8
d(5′C^{p}C^{p}U^p**C**C^{p}U^{p}U^{p}3′)	s-PODN4	−14.9 ± 0.2	−74.3 ± 1.8	−191.5 ± 5.1	76.5
d(5′C^{p}C^{p}U^{p}C^p**C**U^{p}U^{p}3′)	s-PODN5	−14.7 ± 0.2	−73.8 ± 1.4	−190.7 ± 4.2	75.3
d(5′C^{p}C^{p}U^{p}C^{p}C^p**U**U^{p}3′)	s-PODN6	−16.3 ± 0.3	−83.7 ± 2.4	−217.4 ± 6.9	78.0
d(5′C^{p}C^{p}U^{p}C^{p}C^{p}U^p**U**3′)	s-PODN7	−16.4 ± 0.3	−79.7 ± 3.0	−204.1 ± 5.2	80.9

[a] Bases at which substitutions and deletions occur are in bold. [b] See footnotes *a* and *b* from Table 1.

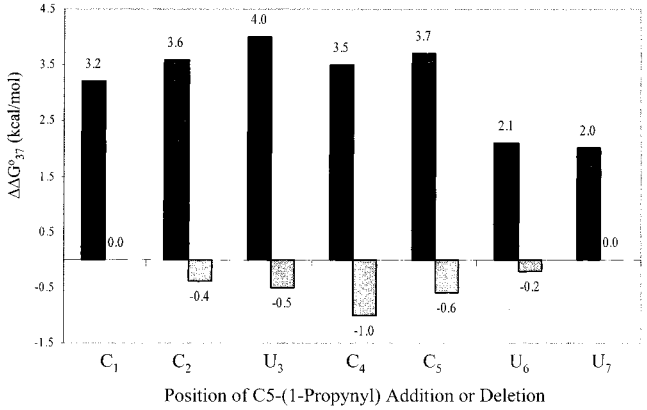

Figure 4. Free energy advantage to the DNA:RNA duplex due to single C5-1-propynyl additions along the DNA strand (gray) compared to the free energy penalty to the PODN:RNA helix due to single C5-1-propynyl deletions along the PODN strand (black). Note that single propynylation at C1 and U7 does not affect duplex stability.

kcal/mol, respectively (Tables 1 and 4). Evidently, the second unpaired nucleotide on each end provides negligible stacking interactions.

Contributions of Single Propynyl Groups to Hybrid Stability in an Otherwise Unmodified DNA Strand. The thermodynamic advantage of propynyl functionalities was elucidated further by making single substitutions in d(5′CCUCCUU3′) (Table 4). These singly substituted strands are referred to as s-DNA*n* oligomers, where *n* is an integer denoting the site of propynyl substitution. The thermodynamic parameters of the unmodified DNA:RNA 11-mer duplex are subtracted from those of the s-DNA*n*:RNA 11-mer duplexes to calculate the thermodynamic advantage of each propynyl substitution. For example,

$$\Delta\Delta G°_{37}(C_4C^p{}_5U_6) = \Delta G°_{37}(\text{s-DNA5:RNA 11-mer}) - \Delta G°_{37}(\text{DNA:RNA 11-mer})$$
$$= -0.6 \text{ kcal/mol} \quad (7)$$

Figure 4 summarizes the changes in free energy for these substitutions at 37 °C. The thermodynamic advantage of these single propynyl substitutions ranges from 0.0 to 1.0 kcal/mol. Substitutions are more stabilizing toward the middle of the helix.

Stability Decrements Due to Deletion of Single Propynyl Groups from an Otherwise Fully Propynylated DNA Strand. The contributions of individual propynyl groups to the stability of the all-propynylated PODN:RNA 11-mer duplex were measured by systematically removing single propynyl groups. These strands are referred to as s-PODN*n* strands, where *n* is an integer denoting the position of propynyl deletion. Table 4 lists the thermodynamic parameters, and Figure 4 summarizes the penalties as calculated from equations equivalent to

$$\Delta\Delta G°_{37}(C^p{}_4C_5U^p{}_6) = \Delta G°_{37}(\text{s-PODN5:RNA 11-mer}) - \Delta G°_{37}(\text{PODN:RNA 11-mer})$$
$$= +3.7 \text{ kcal/mol} \quad (8)$$

Thus, a single propynyl group at dC5 contributes 3.7 kcal/mol to PODN:RNA 11-mer duplex stability, but only 0.6 kcal/mol to s-DNA5:RNA 11-mer duplex stability. On average, a single internal propynyl group stabilizes the PODN:RNA hybrid by 3.4 kcal/mol but stabilizes s-DNAn:RNA 11-mer duplexes by only 0.5 kcal/mol. Deletions toward the 3′ end of the PODN destabilize the PODN:RNA 11-mer duplex less than those toward the 5′ end.

Testing Base-Pairing and Nearest-Neighbor Models for Predicting Stabilities of Y^p-Containing Hybrid Duplexes. Stabilities of DNA:DNA duplexes have been fit to a nearest-neighbor model,[14] but the dependence of stability on the number of GC pairs suggests that stability can be roughly predicted with only a base-pairing model such as that used for DNA polymers.[51,52] In contrast, stabilities of RNA:RNA duplexes can only be predicted well with a nearest-neighbor model.[13] The results summarized in Figure 4 show that the stability increment from a single propynyl group is dependent on whether a fully propynylated duplex is formed. Thus, a simple base-pairing model cannot predict stabilities of Y^p-containing duplexes.

To test the applicability of a nearest-neighbor model to propynylated helices, analogues of d(5′CCUCCUU3′) were synthesized with multiple propynyl substitutions. These are referred to as m-DNA*n*,*o*,*p*'s, where *n*, *o*, and *p* denote the positions of propynyl substitutions. The thermodynamic param-

(51) Wetmur, J. G. *Crit. Rev. Biochem. Mol. Biol.* **1991**, *26*, 227−259.
(52) Blake, R. D.; Bizzaro, J. D.; Blake, J. D.; Delcourt, S. G.; Knowles, J.; Marx, K. A.; SantaLucia, J., Jr. *Bioinformatics* **1999**, *15*, 370−375.

Table 5. Thermodynamic Parameters of m-DNA Strands Bound to 3′-GA**GGAGGAA**AU-5′ [a,b]

		$1/T_M$ plots			
	reference symbol	$\Delta G°_{37}$ (kcal/mol)	$\Delta H°$ (kcal/mol)	$\Delta S°$ (eu)	T_m (°C)
d(5′CCUCC**U^{p}U^p**3′)	m-DNA6,7	−10.4 ± 0.1	−64.6 ± 1.7	−174.6 ± 5.3	56.9
d(5′**C^{p}C^p**UCCUU3′)	m-DNA1,2	−11.1 ± 0.2	−68.3 ± 3.1	−184.4 ± 9.4	59.3
d(5′C**C^p**UC**C^p**UU3′)	m-DNA2,5	−11.4 ± 0.2	−67.3 ± 2.3	−180.4 ± 6.9	61.0
d(5′CCU**C^{p}C^p**UU3′)	m-DNA4,5	−11.8 ± 0.3	−77.2 ± 4.7	−211.1 ± 14.2	59.6
d(5′**C^{p}C^p**U**C^{p}C^p**UU3′)	m-DNA1,2,4,5	−12.6 ± 0.1	−71.6 ± 1.7	−190.2 ± 5.1	65.8
d(5′**C^{p}C^{p}U^{p}C^{p}C^p**UU3′)	m-DNA1,2,3,4,5	−13.4 ± 0.3	−70.1 ± 3.0	−183.0 ± 8.7	70.6

[a] Bases at which C5-1-propyne substitutions occur are in bold. [b] See footnotes *a* and *b* from Table 1.

Table 6. Thermodynamic Parameters of DNA, PODN, and s-PODNs Bound to r(3′GA**GIAGGAA**AU5′)[a,b]

		$1/T_M$ plots			
	reference symbol	$\Delta G°_{37}$ (kcal/mol)	$\Delta H°$ (kcal/mol)	$\Delta S°$ (eu)	T_m (°C)
d(5′C^{p}C^{p}U^{p}C^{p}C^{p}U^{p}U^{p}3′)	PODN	−14.5 ± 0.7	−75.5 ± 6.2	−196.7 ± 8.0	73.8
d(5′CCUCCUU3′)	DNA	(−7.9 ± 0.1)	(−62.7 ± 3.7)	(−176.6 ± 11.0)	44.3
d(5′C^{p}C^{p}U^p**C**C^{p}U^{p}U^{p}3′)	s-PODN4	−13.9 ± 0.4	−81.5 ± 3.7	−217.9 ± 10.9	67.9
d(5′C^{p}C^{p}U^{p}C^p**C**U^{p}U^{p}3′)	s-PODN5	−13.5 ± 0.3	−77.2 ± 3.2	−205.5 ± 9.5	67.8

[a] Positions of C5-(1-propyne) deletions within the PODN strand are in bold. [b] See footnotes *a* and *b* from Table 1.

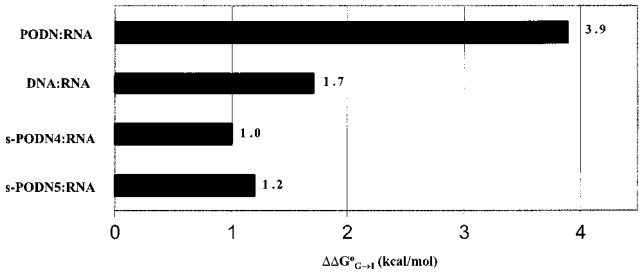

Figure 5. Changes in $\Delta G°_{37}$ of duplex formation upon a G-to-I substitution to give r(3′GA**GIAGGAA**AU5′) in PODN:RNA, DNA:RNA, s-PODN4:RNA, and s-PODN5:RNA duplexes.

eters for binding these m-DNA*n,o,p* strands to r(3′GA**GGAGGAA**AU5′) are listed in Table 5. Comparisons of these thermodynamics indicate that a nearest-neighbor model is also inadequate for predicting stabilities of propynylated hybrid duplexes. For example, the only difference between d(5′**C^{p}C^{p}U^{p}C^{p}C^p**UU3′) and d(5′**C^{p}C^{p}U**C^{p}C^p**UU3′) is a propynyl deletion at U_3. Comparing $\Delta G°_{37}$[m-DNA1,2,3,4,5] with $\Delta G°_{37}$[m-DNA1,2,4,5] shows that removing the propynyl group at U_3 destabilizes the m-DNA1,2,3,4,5:RNA 11-mer duplex by 0.8 kcal/mol. In contrast, removing the propynyl group at U_3 destabilizes the fully propynylated PODN:RNA 11-mer duplex by 4.0 kcal/mol, even though the change in base pairing and nearest neighbors is exactly the same as for the m-DNA1,2,3,4,5:RNA 11-mer duplex. Thus, a nearest-neighbor model is not sufficient to explain effects of propynylation on duplex stability.

Effect of Removing an Amino Group from a Single Guanosine. An inosine substitution for G_6 to give r(3′$\underline{G}_9\underline{A}_8$-**G$_7G_6A_5G_4G_3A_2A_1$**$\underline{A}_{-1}\underline{U}_{-2}$5′) replaces the amino group of G with a hydrogen and therefore eliminates a G_6(amino)−C_2-(carbonyl) hydrogen bond within a duplex. Thermodynamic parameters of duplexes with the inosine substitution are listed in Table 6. Comparison with Table 4 shows that the single G-to-I substitution reduces stability at 37 °C by 3.9 kcal/mol for the PODN:RNA duplex, but by only 1.7, 1.0, and 1.2 kcal/mol, respectively, for the DNA:RNA, s-PODN4:RNA, and s-PODN5:RNA duplexes (Figure 5). Thus, the stability of the PODN:RNA duplex is very sensitive to the presence of the amino group on G_6 and presumably its hydrogen bond, but removal of even a single propynyl group two or three base pairs away dramatically reduces this sensitivity.

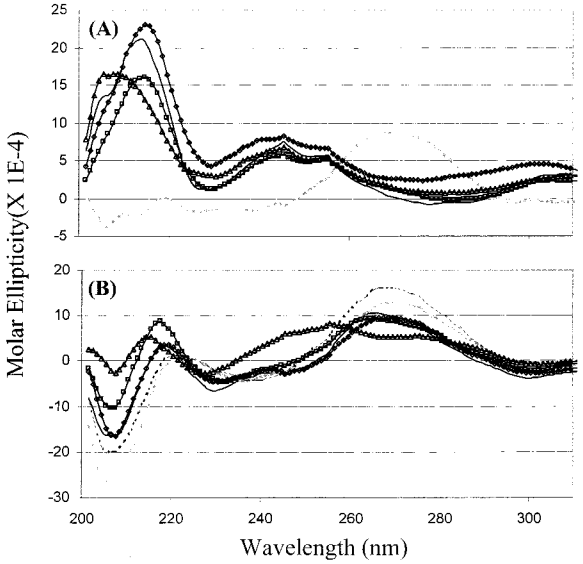

Figure 6. CD spectra at 20 °C for (A) the single strands, 5′-dCCUCCUU-3′ (gray), 5′-dC^{p}C^{p}U^{p}C^{p}C^{p}U^{p}U^p-3′ (black), 5′-d**C**C^p-U^{p}C^{p}C^{p}U^{p}U^p-3′ (△), 5′-dC^{p}C^p**U**C^{p}C^{p}U^{p}U^p-3′ (□), and 5′-dC^{p}C^{p}U^{p}C^{p}C^p-U^p**U**-3′ (◇), as well as (B) the duplexes, 5′-rCCUCCUU-3′:3′-r$\underline{GA}$**GGAGGAA**$\underline{AU}$-5′(---),5′-dCCUCCUU-3′:3′-r$\underline{GA}$**GGAGGAA**$\underline{AU}$-5′ (gray), 5′-dC^{p}C^{p}U^{p}C^{p}C^{p}U^{p}U^p-3′:3′-r$\underline{GA}$**GGAGGAA**$\underline{AU}$-5′ (black), 5′-d**C**C^{p}U^{p}C^{p}C^{p}U^{p}U^p-3′:3′-r$\underline{GA}$**GGAGGAA**$\underline{AU}$-5′ (△), 5′-dC^{p}C^p**U**C^{p}C^p-U^{p}U^p-3′:3′-r$\underline{GA}$**GGAGGAA**$\underline{AU}$-5′ (□), and 5′-dC^{p}C^{p}U^{p}C^{p}C^{p}U^p**U**-3′:3′-r$\underline{GA}$**GGAGGAA**$\underline{AU}$-5′ (◇). Spectra were smoothed over a 5 nm window with a Savitzky−Golay filter.[86]

Circular Dichroism. Figure 6A shows CD spectra of the DNA and PODN single strands. The CD spectrum of the DNA single strand has a large positive band at 270 nm. In contrast, the CD spectrum of the PODN has a large positive band at 245 nm and a larger positive band at 215 nm. Spectral differences can be quantified in a single number, the normalized absolute ellipticity difference (NAED), defined as

$$\mathrm{NAED} = 100(\sum^{\lambda}|[\theta]_1 - [\theta]_2|_\lambda)/(\sum^{\lambda}|[\theta]_1|_\lambda + |[\theta]_2|_\lambda) \quad (9)$$

Here, λ is the wavelength at which the molar ellipticities for systems 1 and 2, $[\theta]_1$ and $[\theta]_2$, were measured. A large NAED reveals dissimilarity in the CD spectra. The average standard error of NAED comparisons is given by the NAED between

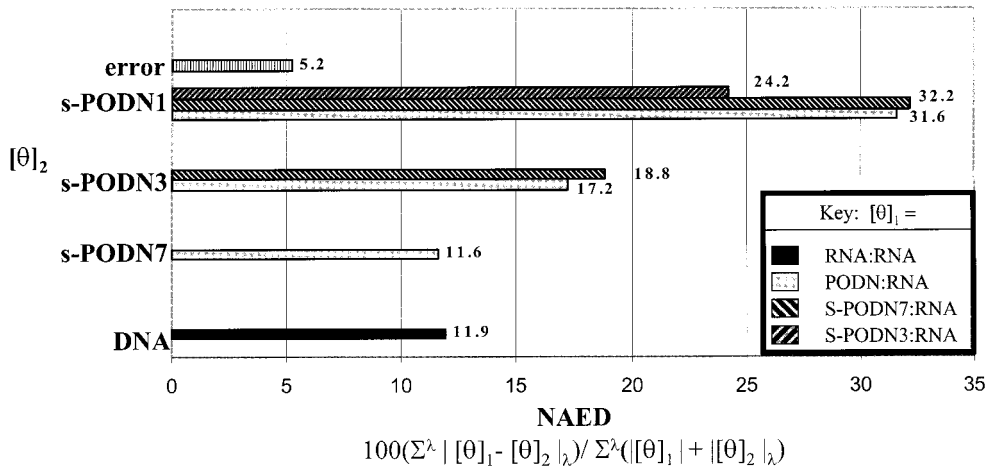

Figure 7. Normalized absolute ellipticity differences (NAEDs) calculated between various duplexes formed with 3′-rGA**GGAGGAA**AU-5′. [θ_1] is for the indicated reference duplex formed with 3′-rGA**GGAGGAA**AU-5′. For example, the bar with a value of 11.9 and labeled DNA quantifies the differences between the CD spectra of the 5′-dCCUCCUU-3′:3′-′-rGA**GGAGGAA**AU-5′ and 5′-rCCUCCUU-3′:3′-rGA**GGAGGAA**AU-5′ duplexes.

two CD spectra collected on the same system at different times. This was performed for each system, and the results were averaged. The average error is 5.2, so any NAED > 5.2 is considered significant. The NAED between the DNA and PODN single strands is 81.9, which is very high, as expected on the basis of inspection of the CD spectra in Figure 6A. The NAED between the DNA:RNA 11-mer and PODN:RNA 11-mer duplexes is 30.0, indicating that there are also significant differences between the CD spectra of these hybrids. Substantial spectral shifts in the absorbance spectra of the DNA and PODN single strands presumably contribute to the NAED (see Supporting Information).

A CD spectrum of the RNA:RNA duplex, r(5′CCUCCUU3′):r(3′GA**GGAGGAA**AU5′), was obtained as a representative of A-form helix geometry. It has a positive and a negative band at 270 and 205 nm, respectively (Figure 6B). These two bands generally distinguish the A-form RNA:RNA helix from the B-form DNA:DNA helix.[53,54] The CD spectrum of the DNA:RNA 11-mer duplex is similar to that of the A-form helix, $NAED_{RNA} = 11.9$, consistent with the geometry of pyrimidine-rich DNA:purine-rich RNA duplexes being similar to A-form.[55−59]

The CD spectra of d(5′C^{p}C^{p}**U**C^{p}C^{p}U^{p}U^{p}3′) and d(5′C^{p}C^{p}-U^{p}C^{p}C^{p}U^{p}**U**3′) are similar to the CD spectrum of the PODN single strand (Figure 6A), $NAED_{PODN} = 15.6$ and 11.4, respectively. The CD spectrum of the d(5′**C**C^{p}U^{p}C^{p}C^{p}U^{p}U^{p}3′) single strand, however, is relatively different, $NAED_{PODN} = 33.0$ (see Supporting Information). If the single-stranded PODN is structured, then the effects of propynyl deletion on this structure may be position-dependent.

CD spectra were measured for various other duplexes to test the impact of single propynyl deletions on the global helix geometry of the PODN:RNA 11-mer duplex (Figure 6B). CD spectra of the s-PODN3:RNA 11-mer and s-PODN7:RNA 11-mer duplexes are similar to the CD spectrum of the PODN:RNA 11-mer duplex, NAED = 17.2 and 11.6, respectively. This suggests that at least the s-PODN7:RNA and PODN:RNA duplexes have similar global geometries. The CD spectrum of the s-PODN1:RNA 11-mer duplex d(5′**C**C^{p}U^{p}C^{p}C^{p}U^{p}U^{p}3′):r(3′GA**GGAGGAA**AU5′) is considerably different from that of the PODN:RNA 11-mer duplex, NAED = 31.6 (Figures 6 and 7). This suggests that a single propynyl deletion from a dC^{p} at the 5′ end can have a significant effect on the global helix geometry.

A Model for Predicting Stabilities of Y^{p}-Containing DNA:RNA Duplexes. Neither a base-pairing nor a nearest-neighbor model is sufficient to account for the effects of propynylation on the stabilities of DNA:RNA duplexes. The following model, however, largely accounts for the observed effects of propynylation:

$$\Delta\Delta G^\circ_i = \Delta G^\circ_i(\text{Y}^{p}\text{-containing duplex}) - \Delta G^\circ_i(\text{unmodified duplex})$$

$$= x_i\Delta G^\circ_{37}(\text{int Y}^{p}\text{ bonus}) + y_i\Delta G^\circ_{37}(\text{5′ dangling end bonus}) + z_i\Delta G^\circ_{37}(\text{cooperativity bonus}) \quad (10)$$

where x_i, y_i, and z_i are the number of times that a particular motif occurs within duplex i. The data for 21 Y^{p}-containing duplexes and the unmodified duplex, d(5′CCUCCUU3′):r(3′GA**GGAGGAA**AU5′), were fit to eq 10 by multiple linear regression (see Supporting Information). Therefore, the model has $f = 22 - 3 - 1 = 18$ degrees of freedom. Although the y-intercept of eq 10 should be zero because the unmodified DNA:RNA duplex is included in the data set, it was not forced to zero in order to allow for small errors (±0.5 kcal/mol) in the ΔG°_{37} of DNA:RNA duplexes. Overall, the model explains the data very well, $R^2 = 0.99$ and rmsd = 0.29 kcal/mol. The duplex, d(5′C^{p}C^{p}U^{p}C^{p}C^{p}U^{p}U^{p}3′):r(3′GAGGAGGAAAU5′), was not included in the fit because it is the only such duplex with seven propynyl groups.

One parameter, ΔG°_{37}(int Y^{p} bonus), accounts for the increased stability of duplexes per nonterminal propynylated

(53) Gray, D. M.; Hamilton, F. D.; Vaughan, M. R. *Biopolymers* **1978**, *17*, 85−106.
(54) Gray, D. M.; Liu, J.-J.; Ratliff, R. L.; Allen, F. S. *Biopolymers* **1981**, *20*, 1337−1382.
(55) Salazar, M.; Fedoroff, O. Y.; Miller, J. M.; Ribeiro, N. S.; Reid, B. R. *Biochemistry* **1993**, *32*, 4207−4215.
(56) Hung, S. H.; Yu, Q.; Gray, D. M.; Ratliff, R. L. *Nucleic Acids Res.* **1994**, *22*, 4326−4334.
(57) Ratmeyer, L.; Vinayak, R.; Zhong, Y. Y.; Zon, G.; Wilson, W. D. *Biochemistry* **1994**, *33*, 5298−5304.
(58) Lesnik, E. A.; Freier, S. M. *Biochemistry* **1995**, *34*, 10807−10815.
(59) Gyi, J. I.; Conn, G. L.; Lane, A. N.; Brown, T. *Biochemistry* **1996**, *24*, 12538−12548.

pyrimidine. Multiple linear regression analysis estimates that each internal Y^p stabilizes a DNA:RNA duplex by 0.99 ± 0.06 kcal/mol at 37 °C. This parameter has a *t*-statistic of 3.11×10^{-12}, indicating that it is statistically different from zero.

The second parameter, $\Delta G°_{37}$(5′ dangling end bonus), accounts for enhanced stacking interactions of a 5′ unpaired adenosine on the RNA strand. This enhanced stability is applied only to duplexes containing (1) a Y^p at the 3′ end of the DNA strand and (2) propynylation of at least five of the remaining six pyrimidines in the DNA strand. Multiple linear regression analysis estimates that this 5′ dangling end enhancement stabilizes a PODN:RNA duplex by 1.17 ± 0.21 kcal/mol at 37 °C. This parameter has a *t*-statistic of 1.67×10^{-5}, indicating that it is statistically different from zero.

The third parameter, $\Delta G°_{37}$(cooperativity bonus), is used to account for the observations that a few duplexes with at least six Y^p's possess unusually enhanced stability. More specifically, duplexes with the PODN(6-mer), s-PODN7, or s-PODN6 strands are unusually stable. Interestingly, the s-PODN1:RNA 11-mer duplex, which has a very unusual CD spectrum, is not unusually stable. Most propynyl deletions eliminate the long-range cooperative interactions that occur between consecutive Y^p's, but this ability seems dependent upon the number of deletions and the end (5′ or 3′) of the DNA strand at which they occur. Multiple linear regression gives $\Delta G°_{37}$(cooperativity bonus) $= -1.94 \pm 0.23$ kcal/mol at 37 °C. This parameter has a *t*-statistic of 5.09×10^{-8}, indicating that it is statistically different from zero.

Discussion

To target RNA in vivo, antisense oligonucleotides must be modified to optimize cellular penetration, half-life, target affinity, target specificity, and other properties.[60−63] Design of self-assembling nanostructures based on nucleic acid-like compounds relies on knowledge of sequence-specific affinities.[9] Rational optimization of affinity and specificity requires knowledge of the interactions that are important for nucleic acid associations. Previous work has shown that propynylation of pyrimidines increases duplex stability.[24,25] Moreover, the propynylated heptamer, d(5′$C^pC^pU^pC^pC^pU^pU^p$3′), is able to specifically inhibit translation of the SV40 large T antigen in cell culture.[2] As shown in Tables 1 and 2, the propynyl groups on d(5′$C^pC^pU^pC^pC^pU^pU^p$3′) increase the stability of its duplex with r(3′GGAGGAA5′) by 8 kcal/mol at 37 °C. Here, we investigate the sources of this stability enhancement in order to reveal new principles for the design of compounds relying on molecular recognition of nucleic acids.

Propynylation Leads to a Less Favorable Enthalpy Change and a More Favorable Entropy Change for Duplex Formation at 37 °C. After accounting for changes in heat capacity, the enthalpy and entropy changes for duplex formation at 37 °C can be compared (Table 2). The $\Delta H°_{37}$ for the PODN:RNA 7-mer duplex is 10.4 kcal/mol less stabilizing than that of the DNA:RNA 7-mer duplex. The $\Delta S°_{37}$ change is less destabilizing to the PODN:RNA 7-mer duplex by 60.5 eu, corresponding to $310.15(60.5)/1000 = 18.8$ kcal/mol in more favorable free energy at 37 °C. This suggests that the enhanced stability of the fully propynylated 7-mer duplex at 37 °C is due to physical phenomena that affect entropy, such as solvation and/or preorganization within the unpaired DNA single strand.

Stacking Interactions of Terminal Unpaired Adenosines. Stacking is one sequence-dependent interaction that contributes to double-helix stability.[11] Comparisons of duplex stability in the presence and in the absence of unpaired terminal nucleotides provide one measure of stacking interactions.[46,47,64] Moreover, most RNA target sequences lie within very long RNA strands. Therefore, antisense molecular recognition of an RNA target will involve both 5′ and 3′ dangling ribonucleotides that can stabilize the double helix.

In the SV40 TAg mRNA antisense:sense duplex in Figure 1B,[2] d(5′CCUCCUU3′):r(3′GA**GGAGGAA**AU5′), rA_{-1} can 5′ stack upon the rA_1-dU_7 base pair, and rA_8 can 3′ stack upon the rG_7-dC_1 base pair. The thermodynamic contributions of adenosines stacking on terminal base pairs depend on helix geometry (Table 3). In B-form DNA:DNA helices, stacking interactions for the equivalent sequences favor duplex formation at 37 °C by 0.5 and 0.4 kcal/mol, respectively.[65] In A-form RNA:RNA helices, the corresponding values are 0.3 and 1.1 kcal/mol.[11,47,64] For the unmodified d(5′CCUCCUU3′):r(3′GA**GGAGGAA**AU5′) duplex studied here, the 5′ and 3′ dangling rA stacking interactions stabilize the duplex by 0.5 and 1.3 kcal/mol, respectively (Table 3). Evidently, stacking of unpaired adenosines at the ends of this DNA:RNA duplex is similar to stacking at the ends of an A-form RNA:RNA duplex.

The 3′ rA_8 dangling end stacking on the $rG_7-dC^p_1$ base pair stabilizes the propynylated duplex, d(5′$C^pC^pU^pC^pC^pU^pU^p$3′):r(3′GA**GGAGGAA**AU5′), by 0.9 kcal/mol (Table 3). In contrast, the free energy increment of the rA_{-1} 5′ dangling end stacking on the $rA_1-dU^p_7$ base pair stabilizes this PODN:RNA 11-mer duplex by 1.9 kcal/mol (Table 3). Thus, stabilization by the 3′ dangling end rA_8 is similar to that observed with A-form helices, but stabilization by the 5′ end rA_{-1} is more favorable than previously observed for equivalent unmodified sequences in either A- or B-form helices (Table 3). In fact, similar stabilization of a DNA:DNA duplex requires a 5′ unpaired dangling 5-nitroindole or pyrene nucleotide, which stabilize by 1.7 kcal/mol.[66] The results suggest that a structural change is induced by propynylation, perhaps increasing the surface area of face-to-face base stacking at the 5′ end.

Stacking Interactions of Terminal Unpaired Cytosines and C5-(1-Propynyl) Cytosines. An unpaired dC at the 5′ end of the rG_7-dC_1 base pair stabilizes the unmodified DNA:RNA duplex by 0.7 kcal/mol, while an unpaired dC at the 3′ end of the rA_1-dU_7 base pair stabilizes it by 0.2 kcal/mol. As shown in Table 3, these increments are within experimental error of those for A-form RNA:RNA duplexes (0.3 and 0.1 kcal/mol, respectively)[64] and B-form DNA:DNA duplexes (0.5 and 0.2 kcal/mol, respectively).[65,66] Similarly, unpaired dC^p at the 5′ end of the $rG_7-dC^p_1$ base pair stabilizes the modified PODN:RNA duplex by 0.3 kcal/mol, and an unpaired dC^p at the 3′ end of the $rA_1-dU^p_7$ pair stabilizes the duplex by 0.7 kcal/mol. Evidently, propynylation does not substantially affect stacking interactions of the cytosines.

The DNA strand within an unmodified DNA:RNA hybrid duplex typically adapts to the RNA strand, progressing toward a predominantly A-form geometry as the purine content within the RNA strand increases.[55−59] The stacking increments in Table 3 for the unmodified DNA:RNA hybrid are consistent with such observations. The presence of propynyl groups along the major

(60) Milligan, J. F.; Matteucci, M. D.; Martin, J. C. *J. Med. Chem.* **1993**, *36*, 1923−1937.
(61) Agrawal, S.; Iyer, R. P. *Pharmacol. Ther.* **1997**, *76*, 151−160.
(62) Branch, A. D. *Trends Biotechnol Sci.* **1998**, *23*, 45−50.
(63) Crooke, S. T. *Methods Enzymol.* **2000**, *313*, 3−45.
(64) Turner, D. H.; Sugimoto, N.; Freier, S. M. *Annu. Rev. Biophys. Biophys. Chem.* **1988**, *17*, 167−192.
(65) Bommarito, S.; Peyret, N.; SantaLucia, J., Jr. *Nucleic Acids Res.* **2000**, *28*, 1929−1934.
(66) Guckian, K. M.; Schweitzer, B. A.; Ren, R. X.-F.; Sheils, C. J.; Tahmassebi, D. C.; Kool, E. T. *J. Am. Chem. Soc.* **2000**, *122*, 2213−2222.

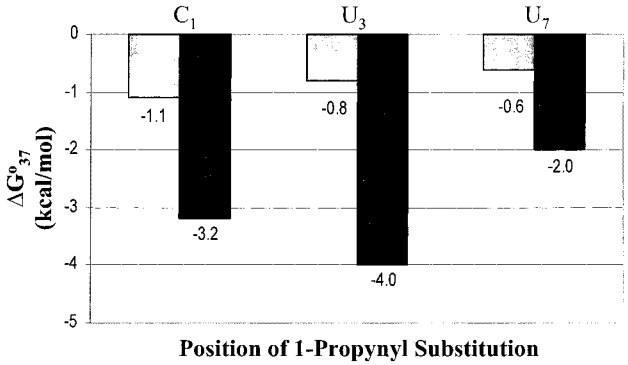

Figure 8. Non-nearest-neighbor thermodynamics of selected propynyl groups. The free energy increment for propynylation at C_1, U_3, and U_7, to form the fully propynylated PODN:RNA hybrid (black), is compared to the corresponding increments to form m-DNA1,2, m-PODN1,2,3,4,5, and m-DNA6,7, respectively (gray).

groove of the PODN:RNA helix, however, changes the relative importance of 5′ and 3′ stacking on both the RNA and DNA strands, suggesting a change in helix geometry.

Effects of Single Propynyl Substitutions and Deletions. The average free energy advantage of single internal Y^p's within the DNA:RNA 11-mer hybrid is 0.5 kcal/mol at 37 °C (Figure 4). This is much less stabilizing than the average advantage of 3.4 kcal/mol obtained by adding a single internal propynyl that results in a fully modified PODN:RNA 11-mer duplex (Figure 4). There is no free energy advantage for adding a single propyne at either end of the DNA:RNA 11-mer helix, but adding a propyne at the 5′ or 3′ end of an otherwise fully propynylated strand provides a free energy advantage of 3.2 or 2.0 kcal/mol, respectively. Thus, the effects of propynylation cannot be explained by a simple base-pairing model.

Preorganization of the unpaired single strand could explain the 0.5 kcal/mol advantage observed for adding a single internal propyne to an otherwise unmodified strand. Preorganization can arise from steric interactions of a bulky propyne within the single strand. For example, if the number of available conformations is reduced 2-fold, then the entropic penalty is more favorable to the free energy of duplex formation by $RT \ln 2 = 0.4$ kcal/mol at 37 °C. The lack of either a 5′ or a 3′ neighbor at the ends of the strand could explain the negligible effect of single propynylation observed at C_1 and U_7.

Long-Range Cooperativity of Multiple Propynyls. The free energy increments associated with propynylating a single pyrimidine are always greater when the fully propynylated PODN:RNA duplex is formed (Figures 4 and 8). For example, propynylation of U_3 to give d(5′**C**^{p}**C**^{p}**U**^{p}**C**^{p}**C**^{p}UU3′) stabilizes the duplex by only 0.8 kcal/mol at 37 °C. Propynylation of U_3 to give d(5′**C**^{p}**C**^{p}**U**^{p}**C**^{p}**C**^{p}**U**^{p}**U**^{p}3′), however, stabilizes the duplex by 4.0 kcal/mol. Similarly, propynylation of C_1 to give d(5′**C**^{p}**C**^{p}-UCCUU3′) or d(5′**C**^{p}**C**^{p}**U**^{p}**C**^{p}**C**^{p}**U**^{p}**U**^{p}3′) stabilizes the duplex by 1.1 and 3.2 kcal/mol, respectively (Figure 8). On average, insertion of a single propynyl group to give the PODN:RNA 11-mer is 2.3 kcal/mol more stabilizing than insertion at the same position in an m-DNA:RNA 11-mer duplex when the fully propynylated duplex is not formed. This reveals highly cooperative long-range interactions between Y^p's.

A Model for Predicting the Stabilities of Y^p-Containing Duplexes. The above results, combined with multiple linear regression, provide a preliminary model for approximate prediction of the enhanced stabilities of Y^p-containing hybrid duplexes. Three parameters are apparently able to account largely for the enhanced stability of such duplexes over those with no propynylation (see eq 10). Although the forces underlying these parameters are not well understood, the model predicts stabilities of 22 hybrids within 0.65 kcal/mol at 37 °C, or better than a factor of 3 in the equilibrium constant for duplex formation. In principle, the model can be combined with nearest-neighbor parameters for unmodified DNA:RNA sequences[16,17] to predict stabilities of other propynylated hybrids.

The first parameter in eq 10, $\Delta G°_{37}$(int Y^p bonus), provides about 1.0 kcal/mol in enhanced stability for each internal Y^p. This may be due to preorganization of the PODN single strand and/or enhanced interstrand stacking interactions of ribo-purine nucleotides promoted by propynyl groups (e.g., as observed for a 5′-terminal unpaired rA). Bases within the confines of a duplex, however, may not have enough conformational freedom to fully optimize stacking, so the stacking effect may not be as large as that observed for dangling ends. Enhanced stacking of Y^p's is unlikely since little or no enhancement is observed for unpaired 5′- and 3′-terminal unpaired propynylated cytosines (Tables 1 and 3).

The second parameter, $\Delta G°_{37}$(5′dangling end bonus), provides about 1.2 kcal/mol in enhanced stability if a 5′ dangling end rA is adjacent to a terminal propynylated base pair in a hybrid with at least six propynyl groups. This value corresponds well with the measured thermodynamic advantage of $1.9 - 0.5 = 1.4$ kcal/mol for the 5′ r$\underline{A}_{-1}$ stacking interaction on the rA_1:dU^p_7 base pair in the PODN:RNA 9-mer duplex (Tables 1 and 3). The magnitude of this parameter will probably be similar for other purines but different for pyrimidines at the 5′ end of the RNA strand, as observed for DNA:DNA[65,66] and RNA:RNA[11,47,64] duplexes. Note that a parameter for 3′ dangling end stacking on the PODN:RNA duplex is not included in the model for stability enhancement because such interactions are relatively insensitive to propynyl substitutions (Tables 1 and 3).

The third parameter, $\Delta G°_{37}$(cooperativity bonus), is estimated to provide about 1.9 kcal/mol in enhanced stability. This parameter accounts for the additional enhanced stability of hybrid duplexes formed by the PODN(6-mer), s-PODN6, and s-PODN7 strands. These duplexes apparently have a common feature that is not accounted for by the first and second parameters. Not enough data are available to provide general rules for this parameter. For the data set, however, cooperativity is observed for helices having at least six propynyl groups, with at least five occurring consecutively and no CC^p or C^{p}C interfaces.

It is also possible that cooperativity is dependent on the side (5′ or 3′) of the DNA strand containing interruptions, rather than or in addition to the sequence at interfaces. Cooperativity is observed when an unmodified U is the penultimate (s-PODN6) or terminal 3′ nucleotide (s-PODN7), but not when an unmodified C is the terminal 5′ nucleotide (s-PODN1). Such an effect could be driven by the very favorable 5′ interstrand stacking of the r$\underline{A}_{-1}$ (Figure 1B and Table 3) discussed previously, which could help maintain a duplex geometry that favors cooperative interactions. The observation of an unusual CD spectrum for the s-PODN1:RNA duplex, where only C_1 is not propynylated, is consistent with the hypothesis that cooperativity is dependent upon helix geometry.

With these parameters, the cooperativity model predicts the free energy of the PODN:RNA 11-mer duplex to be approximately −17.7 kcal/mol, which is 0.7 kcal/mol less stable than measured (Table 4). This suggests that interactions responsible for long-range cooperativity may strengthen as the number of consecutive Y^p's increase within a propynylated DNA strand. In this case, the cooperativity increment grows to −2.6 kcal/mol when seven consecutive Y^p's occur in the DNA strand.

While considerable effort will be required to fully elucidate the sequence and/or length dependence of cooperativity, it is clearly an important effect within propynylated oligonucleotides.

The Enhanced Stability Due to Propynylation Is Greatly Reduced When the Amino Group on a Single Guanosine Is Replaced by Hydrogen. To test the sensitivity of the cooperative interactions to helix composition, inosine was substituted for G_6 to give d(5′CCUCCUU3′):r(3′GA**GIAGGAA**AU5′). Inosine substitution for G in a G−C pair typically results in the loss of 0.5−1.8 kcal/mol in the free energy of RNA:RNA and DNA:DNA duplexes.[67−70] This increment has been assigned to hydrogen bonding of the amino group because essentially equivalent free energy increments are provided by stacking of an unpaired G or I at the end of a helix.[67] Moreover, G and I have similar charge distributions.[71] Theoretical support for attributing G-to-I free energy increments to hydrogen bonding is also provided by molecular modeling of nucleic acids.[72]

Inosine substitution in the DNA:RNA 11-mer duplex makes hybridization less favorable by 1.7 kcal/mol at 37 °C, consistent with previous values for G-to-I substitutions. The same substitution, however, destabilizes the PODN:RNA 11-mer duplex by 3.9 kcal/mol. Apparently, this amino group is 2.2 kcal/mol more stabilizing in the PODN:RNA 11-mer duplex than in the DNA:RNA 11-mer duplex. This difference is similar to the calculated stability contribution of 2.6 kcal/mol for long-range cooperative interactions within the PODN:RNA 11-mer duplex, suggesting that minor groove hydrogen bonds play a role in maintaining such interactions. Alternatively, a different conformation for the PODN:RNA hybrid may prevent hydration of the $C^{p}{}_{2}$ carbonyl left unpaired by removal of the G_6 amino group.

To test if the large effect of amino replacement depends on long-range cooperative interactions due to seven consecutive propynyl groups, the propynyls at C_4 and C_5 were separately removed, and the thermodynamic effects of inosine substitution for G_6 were measured. When C_4 or C_5 is the only unmodified pyrimidine in the strand, the G-to-I substitution reduces duplex stability by only 1.0 and 1.2 kcal/mol, respectively (Figure 5). Thus, the increment is made less favorable by about 2.8 kcal/mol when long-range cooperativity is eliminated by removing a propynyl group. Again, this difference is similar to the 2.6 kcal/mol assigned to long-range cooperativity in the PODN:RNA 11-mer duplex. Evidently, the contribution of the G_6 amino group to duplex stability is coupled strongly to the cooperative interactions between consecutive propynyl groups on the complementary DNA strand. Apparently, such interactions change the environment of the minor groove, in addition to enhancing the overall stability of the hybrid duplex.

Effects of Single Propynyl Deletions on Helical Geometry of the PODN:RNA Duplex. The CD spectra of DNA and PODN single strands are dramatically different, NAED = 81.9 (Figure 6A and Supporting Information). This difference is at least partially due to different optical properties of modified and unmodified pyrimidines (see Supporting Information) but may also indicate that the structures of the unpaired single strands are altered due to propynylation. CD spectra also suggest that the impact of propynyl group deletions on the helical geometry of the PODN:RNA duplex depends on the location of a deletion. The s-PODN7:RNA duplex is missing a propynyl group at the 3′ end of the DNA strand, and its CD spectrum is similar to that of the PODN:RNA duplex, $NAED_{PODN} = 11.6$ (Figure 7). The s-PODN3:RNA duplex is missing a propynyl group near the middle of the duplex, and its $NAED_{PODN} = 17.2$ and $NAED_{s-PODN7} = 18.8$ (Figure 7). NAED comparisons show that the CD spectrum of the s-PODN1:RNA duplex is very dissimilar to that of the PODN:RNA, $NAED_{PODN} = 31.6$, and s-PODN7:RNA duplexes, $NAED_{s-PODN7} = 32.2$ (Figure 7). Interestingly, long-range cooperativity is absent in the s-PODN1:RNA duplex, even though it has six consecutive propynyl substitutions. Therefore, long-range cooperative interactions could be dependent on helical structure. These results suggest that interactions governing helical structure at the 5′ and 3′ ends of the PODN:RNA duplex may not be equal, resulting in an intolerance of propynyl deletions at the 5′ end. This could be due to the large difference in unpaired rA stacking interactions at the 5′ and 3′ ends of the PODN:RNA duplex (Table 3).

Possible Sources of Long-Range Cooperative Interactions. There are many possible sources of long-range cooperative effects in duplexes containing multiple consecutive propynyl groups. The enthalpy change for formation of the fully propynylated duplex is less favorable than that of the unmodified duplex (Table 2). This suggests that base stacking is not more favorable in the propynylated duplex, since base stacking is driven by a favorable enthalpy change.[11,46,49,73] Bulky propynyl substitutions may prevent optimal stacking interactions within PODN:RNA duplexes by restricting conformational space available for propeller twisting, roll, etc. It is possible, however, that base stacking is more favorable in the unpaired propynylated strands because there is more volume exclusion due to multiple propynyl groups. That is, the preorganization effect described above for single propynyl substitutions can accumulate in a cooperative manner for multiple propynyl substitutions. This would make the enthalpy and entropy changes for duplex formation less and more favorable, respectively. Preliminary 1D and 2D NMR spectra of single strands at various temperatures suggest that helical stacking occurs only between propynylated pyrimidines within the PODN, while none occurs within the unmodified DNA.

A classical hydrophobic effect is suggested by the 18.8 kcal/mol more favorable entropy change at 37 °C for PODN:RNA 7-mer duplex hybridization over its unmodified analogue (Table 2). Indeed, the dU^{p} analogue is more hydrophobic than dU.[74] The ΔC°_{p} of the DNA:RNA duplex is more negative than that of the PODN:RNA duplex, however, arguing against a classical hydrophobic effect.[49]

Chalikian et al.[75] have suggested that there is a specific "cooperative patch" of 13 water molecules that lie in the major groove of G−C base pairs and a specific cooperative "spine" of 8 water molecules in the minor groove of A−U base pairs of duplexes in solution. Egli et al.[76] found a cooperative patch of water molecules within the major and minor grooves of a crystal of $r(5'CCCCGGGG3')_2$. They contend that it is 2′ hydroxyl groups of RNA, "which lock the sugar−phosphate backbone in a conformation that allows water to bridge adjacent

(67) Turner, D. H.; Sugimoto, N.; Kierzek R.; Dreiker, S. D. *J. Am. Chem. Soc.* **1987**, *109*, 3783−3785.
(68) Martin, F. H.; Castro, M. M.; Aboul-ela, F.; Tinoco, I., Jr. *Nucleic Acids Res.* **1985**, *13*, 8927−8938.
(69) Aboul-ela, F.; Koh, D.; Tinoco, I., Jr.; Martin, F. H. *Nucleic Acids Res.* **1985**, *13*, 4811−4824.
(70) Kawase, Y.; Iwai, S.; Inoue, H.; Miura, K.; Ohtsuka, E. *Nucleic Acids Res.* **1986**, *14*, 7727−7736.
(71) Burkard, M. E.; Turner, D. H. *Biochemistry* **2000**, *39*, 11748−11762.
(72) Stofer, E.; Chipot, C.; Lavery, R. *J. Am. Chem. Soc.* **1999**, *121*, 9503−9508.
(73) Freier, S. M.; Hill, K. O.; Dewey, T. G.; Marky, L. A.; Breslauer, K. J.; Turner, D. H. *Biochemistry* **1981**, *20*, 1419−1426.
(74) Valko, K.; Fellegbvari, I.; Sagi, J.; Szemzo, A. *J. Liq. Chromatogr.* **1989**, *12*, 2103-2116.
(75) Chalikian, T. V.; Volker, J.; Srinivasan, A. R.; Olson, W. A.; Plum, G. E.; Breslauer, K. J. *Biopolymers* **1999**, *50*, 459−471.
(76) Egli, M.; Portmann, S.; Usman, N. *Biochemistry* **1996**, *35*, 8489−8494.

phosphates". Our data suggest that the enhanced stability of the PODN:RNA duplex is due to the entropic penalty being less destabilizing than for the DNA:RNA duplex. Therefore, cooperative solvent molecules could be excluded from the helix by geometric distortions induced by multiple consecutive bulky hydrophobic propynyl groups, resulting in a more dehydrated major groove. This could lead to a less favorable enthalpy change and a more favorable entropy change for duplex formation. The cumulative bulk of propynyls could also prevent optimal stacking, which may explain a less favorable enthalpy contribution upon full propynylation (Table 2).

Helix distortion and dehydration could also rationalize the large duplex destabilization resulting from removal of the amino group from G_6. This effect may be due to strengthening of the G_6(amino)−C_2(carbonyl) hydrogen bond. This hydrogen bond could be shorter due to bulky propynyl groups in the major groove, affecting parameters such as propeller twist and opening, etc. Also, dehydration of the minor groove would reduce the local dielectric constant. The strength of an electrostatic interaction such as a hydrogen bond is inversely proportional to its length and the medium's dielectric constant. A reduction in either or both parameters will lead to an increase in the strength of the G(amino)−C(carbonyl) hydrogen bonds. When one of the propynyl groups is eliminated, as in d(5′C^{p}C^{p}U^{p}-**C**C^{p}U^{p}U^{p}3′) or d(5′C^{p}C^{p}U^{p}C^{p}**C**U^{p}U^{p}3′), the duplex conformation and hydration may change, causing the apparent strength of the minor groove hydrogen bond to revert back to that in the unmodified DNA:RNA helix. Alternatively, the strength of the hydrogen bond in the duplex may not be affected, but the conformation of the fully propynylated duplex may prevent hydration of the unpaired carbonyl on a C^{p} opposite an inosine. Both possibilities require that propynyls cooperatively induce a global change in helix conformation.

Impact of Enhanced Cooperative Interactions on Affinity and Specificity of Binding. Propynylation of seven consecutive pyrimidines leads to highly cooperative binding of d(5′C^{p}C^{p}-U^{p}C^{p}C^{p}U^{p}U^{p}3′) to r(3′GA**GGAGGAA**AU5′), which drastically increases the potency of the antisense:sense interaction by 8.8 kcal/mol at 37 °C (Table 4). Most of the enhanced stability is focused within the base-pairing region since the contribution of stacked unpaired dangling ends is only 1 kcal/mol more favorable for the fully propynylated duplex.

It has been proposed that the sequence r(3′GA**GG-AGGAA**AU5′) exists within a stable 27-nucleotide stem loop structure within the SV40 TAg mRNA,[2] and it is therefore surprising that d(5′C^{p}C^{p}U^{p}C^{p}C^{p}U^{p}U^{p}3′) is able to inhibit translation of this mRNA. The results presented here show that the free energy of base pairing for the fully propynylated oligonucleotide is sufficient to allow it to invade RNA targets buried within stable intramolecular secondary structures. Such properties of short PODNs could be used to destroy secondary structures, as well as tertiary contacts, that are crucial for a target RNA's function. Probing for sequences without regard to RNA structure can lead to false-negative results in molecular beacon[5,77−79] and microarray assays[4,80−85] if the target sequences are buried within highly stable local secondary structures. The highly cooperative nature of consecutive propynylated pyrimidines could unmask such sequences.

The non-nearest-neighbor interactions that enhance the cooperativity of PODN:RNA hybridization may also increase an antisense PODN's target specificity. Small changes, such as propyne group deletions and elimination of an amino group, greatly destabilize the antisense:sense complex. Thus, larger changes, such as mismatches, may cause even greater destabilization of the complex. Therefore, the antisense PODN might have high specificity for its intended target due to a loss of long-range cooperative interactions when paired with mismatched bystander targets. This could facilitate applications such as antisense-based drugs,[60−63] microarray screening,[4,80−85] molecular beacon probing,[4,77−79] and design of self-organizing nanostructures that rely on nucleic acid-based molecular recognition.[7−9]

Acknowledgment. The authors thank D. H. Mathews, Professor S. M. Testa, Professor T. R. Krugh, S. J. Schroeder, and Professor S. Mukamel for helpful discussions. We also thank Drs. M. D. Matteucci and B. C. Froehler for sparking our interest in this system and sharing results prior to publication. This research was funded in part by NIH Grant GM22939. T. W. Barnes III is a Sherman-Clark Fellow, Arnold Weissberger Memorial Fellow, and Oral Cellular and Molecular Biology Training Scholar (PHS Grant No. DE07202-10).

Supporting Information Available: NAED comparisons for single strands, absorbance spectra of single strands, thermodynamic parameters from averaging melting curves and from $1/T_M$ vs ln(C_T) plots for all duplexes, multiple linear regression analysis scoring, and resultant model parameters (PDF). This material is available free of charge via the Internet at http://pubs.acs.org.

JA003208T

(77) Sokol, D. L.; Zhang, X.; Lu, P.; Gewirtz, A. M. *Proc. Natl. Acad. Sci. U.S.A.* **1998**, *95*, 11538−11543.
(78) Bonnet, G.; Tyagi, S.; Libchaber, A.; Kramer, F. R. *Proc. Natl. Acad. Sci. U.S.A.* **1999**, *4*, 6171−6176.
(79) Liu, X.; Tan, W. *Anal. Chem.* **1999**, *71*, 5054−5059.
(80) Healey, B. G.; Matson, R. S.; Walt, D. R. *Anal. Biochem.* **1997**, *251*, 270−279.
(81) Hacia, J. G.; Woski, S. A.; Fidanza, J.; Edgemon, K.; Hunt, N.; McGall, G.; Fodor, A. P. A.; Collins, F. S. *Nucleic Acids Res.* **1998**, *26*, 4975−4982.
(82) Maldonado-Rodriguez, R.; Espinosa-Lara, M.; Loyola-Abitia, P.; Beattie, W. G.; Beattie, K. L. *Mol. Biotechnol.* **1999**, *11*, 13−25.
(83) Gerry, N. P.; Witowski, N. E.; Day, J.; Hammer, R. P.; Barany, G.; Barany, F. *J. Mol. Biol.* **1999**, *292*, 251−262.
(84) Chen, D.; Yan, Z.; Cole, D. L.; Srivatsa, G. S. *Nucleic Acids Res.* **1999**, *27*, 389−395.
(85) Walt, D. R. *Science* **2000**, *287*, 451−452.
(86) Press, W. H.; Teukolsky, S. A.; Vetterling, W. T.; Flannery, B. P. *Numerical Recipes in C*, 2nd ed.; Cambridge Univeristy Press: Cambridge, England, 1992.